Journal of Bio- and Tribo-Corrosion (2018) 4:34
https://doi.org/10.1007/s40735-018-0152-1

Kinetic–Thermodynamic Properties of a Polyacrylamide on Corrosion Inhibition for C-Steel in 1.0 M HCl Medium: Part 2

M. Beniken[1] · M. Driouch[1] · M. Sfaira[1] · B. Hammouti[2] · M. Ebn Touhami[3] · M. Mohsin[4]

Received: 9 February 2018 / Revised: 6 May 2018 / Accepted: 7 May 2018 / Published online: 17 May 2018

Abstract
In this second part, the adsorption and thermodynamics properties of a polyacrylamide PA on corrosion inhibition of in 1.0 M HCl solution were analyzed by means of potentiodynamic polarization and electrochemical impedance spectroscopy techniques. Besides, the effects of temperature as well as the immersion time, on the inhibition efficiency, at 3×10^{-6} mol L^{-1} of PA, were also investigated. The adsorption data were modeled using six linearized forms of adsorption isotherms corresponding to Langmuir, Flory–Huggins, Temkin, Frumkin, Freundlich as well as the kinetic–thermodynamic model of El-Awady. The Langmuir model was first ruled out notwithstanding the highest value of linear regression coefficient and a slope close to unity. Secondly, it was found, according to both El-Awady and Flory–Huggins models, that exactly three molecules of water were replaced by one PA molecule. Thirdly, it was shown the presence of repulsive lateral interactions in the adsorbed inhibitory layer confirmed by the negative sign of the interaction parameters of Temkin and Frumkin isotherms. The effect of immersion period revealed significant improvement of the charge transfer resistance and accordingly the inhibiting efficiency which reach circa 96% after 6 h. The confrontation of thermodynamic (K_{ads}, $\Delta_r G_{ads}^{\circ}$) along with the kinetic parameters (A, E_a) showed that the adsorption of PA molecules onto C-steel surface involved both chemical and physical adsorption but predominantly chemisorption.

Keywords Polyacrylamide · Adsorption · Isotherms · Lateral interactions · Immersion time

1 Introduction

It is a well-known fact that C-steel, due to its availability, low cost and its particular and unique properties, is especially recommended, compared to other materials, in various fields of technology where it is frequently intentionally or unintentionally exposed to acid solutions. However, C-steel is susceptible to corrosion in acid media. On the other hand, the high cost of C-steel corrosion affects numerous industries, domestic applications, and public sectors worldwide then highlights the need for improved effective corrosion inhibition.

It has been shown that the polymers manifest excellent corrosion inhibition which has attracted several researchers due to their abundantly use, cost effectiveness, as well as eco-friendliness in addition to their inherent stability and multiple adsorption centers [1]. Some recent reports on the successful use of homopolymers such as polyacrylamide [2], polyvinylpyrrolidone [3], polyacrylic acid [4], polyethyleneimine [5], polyaniline [6], polyvinylpyridine [7], and polyvinyl imidazoles as corrosion inhibitors can be found in the literature [8, 9]. Besides, the employ of copolymers such as styrene–maleic acid and maleic acid–styrene–acrylic ester terpolymer as inhibitors has also been reported [10, 11]. In addition, studies conducted, in the literature, on corrosion inhibition with polymers, have concerned not only C-steel

✉ M. Beniken
mustapha.beniken@yahoo.fr

1 Laboratoire d'Ingénierie des Matériaux, de Modélisation et d'Environnement (LIMME), Faculté des Sciences, Université Sidi Mohamed Ben Abdellah, USMBA, B.P. 1796, 30000 Atlas – Fès, Morocco

2 LCAE–URAC18, Faculté des Sciences, Université Mohamed Premier, BP 717, 60000 Oujda, Morocco

3 Laboratoire d'Ingénierie des Matériaux et Environnement : Modélisation et Application (LIMEMA), Faculté des Sciences, Université Ibn Tofaïl, B.P. 133, 14000 Kenitra, Morocco

4 Department of Chemistry, University of Sharjah, P.O. Box 27272, Sharjah, United Arab Emirates

but several metals such as aluminum and zinc in various aqueous environments [1–20].

Generally, corrosion inhibitors are found to protect steel corrosion in acid solutions by adsorption. These inhibitors act at the metal–solution interface and replace water molecules. The improved performance of polymers is related to the fact that a single polymeric chain displaces, thanks to the large repeating units of its bulky structure, many water molecules from the metal surface, thus making the adsorption process entropically favorable along with the presence of multiple bonding sites which makes the desorption of polymers a slower process. Furthermore, the corrosion inhibition activity of polymers could be due to their ability to form complexes with metal ions, through their functional groups, which occupy large area, thereby blanketing the surface and protecting the metals against corrosive agents present in solution [1]. The kind of interaction between the inhibitor and metallic surface can be provided by thermodynamic adsorption parameters deducted from the adsorption isotherm results, along with kinetic corrosion parameters linked to the effects of temperature and immersion time. The adsorption may be physisorption, chemisorption or a combination of both.

The present work is a continuation of the previous work concerning the study on inhibition efficiency of polyacrylamide (PA) (Fig. 1) on corrosion of C-steel in 1.0 M HCl. In fact, in the previous work (part 1), the experimental conditions of PA synthesis with high molecular weight have been specified and the results of characterization of its chemical structure by different spectroscopic techniques were presented. The inhibitive action of PA on corrosion of C-steel in 1.0 M HCl has been investigated at different concentrations and at 298 K using mass-loss (ML), potentiodynamic polarization (PP), and electrochemical impedance spectroscopy (EIS) techniques. A very good concordance was obtained from the three techniques. PA was mixed-type inhibitor with predominant control of anodic reaction. The adsorption of PA was established by both physical and chemical interactions of non-protonated and protonated molecules. The inhibition efficiency of PA was slightly ameliorated in 0.5 M H_2SO_4 at 298 K.

The present work (Part 2) illustrates the evaluation of kinetic activation and adsorption parameters referring to the studies of both effects of temperature as well as immersion time period investigated by means of PP and EIS techniques. In addition, different adsorption isotherms at 298 K are considered. A confrontation of these isotherms is conducted in order to develop the most probable mechanism of PA adsorption onto C-steel in terms of number of water molecules to be substituted by one PA molecule, the presence or not of interaction between adsorbed PA molecules and its nature.

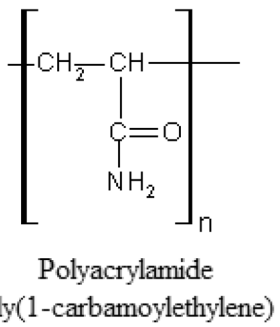

Fig. 1 Chemical structure of PA repeat unit

2 Experimental Details

2.1 Materials and Methods

2.1.1 Materials

The C-steel samples, containing in wt%: 0.210% C, 0.360% Si, 1.250% Mn, 0.046% S, 0.025% P, 0.160% Cr, 0.160% Ni, 0.081% V, 0.017% Sn, 0.410% Cu, 0.003% Al, 0.017% Mo, and the remainder iron Fe, were prepared by the conventional method widely reported in the literature [21]. Appropriate concentrations of PA inhibitor in aggressive solutions of 1.0 M HCl were prepared to perform the measurements.

2.1.2 Electrochemical Tests

Electrochemical measurements were carried out in a conventional three-electrode glass cell and were conducted by a potentiostat/galvanostat (Radiometer-analytical PGZ 100) and controlled with analysis software (Voltamaster 4). The working electrode was used as a rectangular specimen of C-steel with only one face of the electrode with a constant 1 cm^2 surface area exposed. Ag/AgCl (3 M KCl) was used as reference electrode, and a rectangular platinum foil was used as counter electrode. The working electrode was immersed in 50 mL of the test solution during 30 min until a quasi-steady state of the open circuit potential (E_{ocp}) was achieved. Polarization curves were recorded by scanning the electrode potential at first in the cathodic direction from − 900 to E_{ocp} + 20 $mV_{Ag/AgCl}$ and then in the anodic direction from E_{ocp} − 20 $mV_{Ag/AgCl}$ to − 100 mV with the same scanning rate of 1 mV s^{-1}. The corrosion parameters such as cathodic Tafel slope (β_c), corrosion current density (i_{corr}) and corrosion potential (E_{corr}) were evaluated by using Ec-Lab software.

Impedance spectra were recorded, at the open circuit potential, in the frequency range, from 100 kHz to 100 mHz with 10 points per decade, at alternating current amplitude of ± 10 mV ac voltage peak-to-peak. The impedance spectra, given in the

Nyquist and Bode representations, were analyzed in terms of an appropriate equivalent electrical circuit implemented in the Ec-Lab software.

3 Results and Discussion

3.1 Adsorption Isotherms

The adsorption isotherm experiments are performed to have more insights into the mechanism of corrosion inhibition, since they describe the molecular interaction of inhibitor molecules with the active sites on C-steel surface [22]. Given that, the solvent water molecules, in uninhibited medium, first adsorb at the metal/solution interface. So, in inhibited medium, the adsorption of organic inhibitor molecules can be regarded as a quasi-substitution process between the organic compound in the aqueous solution $Org_{(sol)}$ and the water molecules already adsorbed on the metallic surface $H_2O_{(ads)}$ as shown in Eq. (1):

$$Org_{(sol)} + xH_2O_{(ads)} \leftrightarrow Org_{(ads)} + xH_2O_{(sol)} \quad (1)$$

where x is the size factor ratio representing the number of water molecules replaced by one molecule of organic inhibitor. It is assumed to be independent of coverage or charge on the electrode [23].

The degree of surface coverage (θ), which represents the part of the metal surface covered by inhibitor molecules, suggests that a barrier is formed between the metal atoms and the corrosive medium. The molecules may be adsorbed at the metal/solution interface by the formation of either electrostatic or covalent bonds between the adsorbates and the metal surface atoms.

In the present study, values of θ, corresponding to different concentrations of PA at 298 K, given in Table 1, are easily determined from mass-loss (θ_{ML}), potentiodynamic polarization curves (θ_{PP}) and electrochemical impedance spectroscopy (θ_{EIS}) methods. These values are calculated in each case by the ratio $\eta\%$ /100 if one assumes that the values of $\eta\%$ do no differ substantially from θ, according to Eqs. (2), (3), and (4), respectively:

$$\theta_{ML} = 1 - \left(W_{corr,\,inh}/W_{corr,\,0}\right) = \eta_{ML}\%/100 \quad (2)$$

$$\theta_{PP} = 1 - \left(i_{corr,\,inh}/\,i_{corr,\,0}\right) = \eta_{PP}\%/100 \quad (3)$$

Table 1 Surface coverage degree obtained from mass-loss (θ_{ML}), potentiodynamic polarization (θ_{PP}), and electrochemical impedance spectroscopy (θ_{EIS}) methods for C-steel in 1.0 M HCl at different concentrations of PA inhibitor at 298 K

C_{inh} (mol L^{-1})	θ_{ML}	θ_{PP}	θ_{EIS}
1×10^{-6}	0.806	0.789	0.792
2×10^{-6}	0.840	0.835	0.832
3×10^{-6}	0.862	0.851	0.852
4×10^{-6}	0.869	0.855	0.853

$$\theta_{EIS} = 1 - \left(\left(1/R_{ct,\,inh}\right)/\left(1/\,R_{ct,\,0}\right)\right) = \eta_{EIS}\%/100 \quad (4)$$

The most commonly used adsorption isotherms are tested to fit the experimental data, such as Langmuir, Flory–Huggins, Temkin, Frumkin, Freundlich as well as the kinetic–thermodynamic model of El-Awady. Indeed, electrochemical systems are often referred either to ideal or non-ideal adsorptions because of the different assumptions on which each adsorption isotherm is based. All these isotherms obey a common general expression given below by Eq. (5) [24]:

$$f(\theta,\,x)\,\exp\left(-2a\theta\right) = K_{ads}C_{inh} \quad (5)$$

where $f(\theta, x)$ is the configurational factor which depends upon the physical model and the assumptions underlying the derivation of the isotherm; C_{inh} is the inhibitor concentration in the electrolyte; a is the molecular interaction parameter depending on the molecular interactions in the adsorption layer and on the degree of heterogeneity of the surface, and K_{ads} is the equilibrium constant of the adsorption process which is temperature dependent and it is related to the free energy of adsorption according to Eq. (6):

$$\Delta_r G_{ads}^{\circ} = -RT\,\ln\left(55.5\,K_{ads}\right) \quad (6)$$

where R is the universal gas constant ($R = 8.314$ J K^{-1} mol^{-1}) and T is the thermodynamic temperature (K). In the above equation, 55.5 mol $L^{-1}$is used for molar concentration of water in solution.

In fact, all these isotherms can be described by their conventional and linear forms as shown in Table 2.

Figure 2 shows the linear fit according to the three curves derived from gravimetric and electrochemical techniques. The choice of PA concentrations was limited up to 4×10^{-6} mol L^{-1} because any further increase of PA concentration was found to deviate from the tested adsorption isotherms (data not reported here). On the basis of the three previous methods, the adsorption parameters deduced from the different isotherms and values of the determination coefficient R^2 are recorded in Table 3.

Table 3 shows that the best fit is obtained with the use of Langmuir adsorption isotherm with regression coefficient R^2 of 0.9999, whereas the slope of the corresponding equation deviates slightly from unity. Accordingly, the Langmuir model seems to be suitable to describe the adsorption process as usually reported by several researchers [25, 26].

However, such deviation may take its roots from the Langmuir assumptions certainly not respected. In fact, the Langmuir model remains hypothetical and often referred to an ideal adsorption which is not really applicable in concrete electrochemical systems. For this reason, in the present study, we were obliged to look for other isotherm models taking into account the non-ideal character of the

Table 2 Conventional and linear forms of the most commonly used adsorption isotherms

Isotherm	Conventional form	Linear form
Langmuir	$\theta/1-\theta = K_{ads}C_{inh}$	$C_{inh}/\theta = 1/K_{ads} + C_{inh}$
El-Awady	$(\theta/1-\theta)^{1/y} = K_{ads}C_{inh}$	$\log(\theta/1-\theta) = y\log(K_{ads}) + y\log(C_{inh})$
Flory–Huggins	$\theta/x(1-\theta)^x = K_{ads}C_{inh}$	$\log(\theta/C_{inh}) = \log(xK_{ads}) + x\log(1-\theta)$
Temkin	$\exp(-2a\theta) = K_{ads}C_{inh}$	$\theta = -1/2a\ln(K_{ads}) + -12a/\ln(C_{inh})$
Frumkin	$(\theta/1-\theta)\exp(-2a\theta) = K_{ads}C$	$\ln(\theta/C_{inh}(1-\theta)) = \ln(K_{ads}) + 2a\theta$
Freundlich	$\theta = K_{ads}(C_{inh})^n$	$\ln\theta = \ln(K_{ads}) + n\ln(C_{inh})$

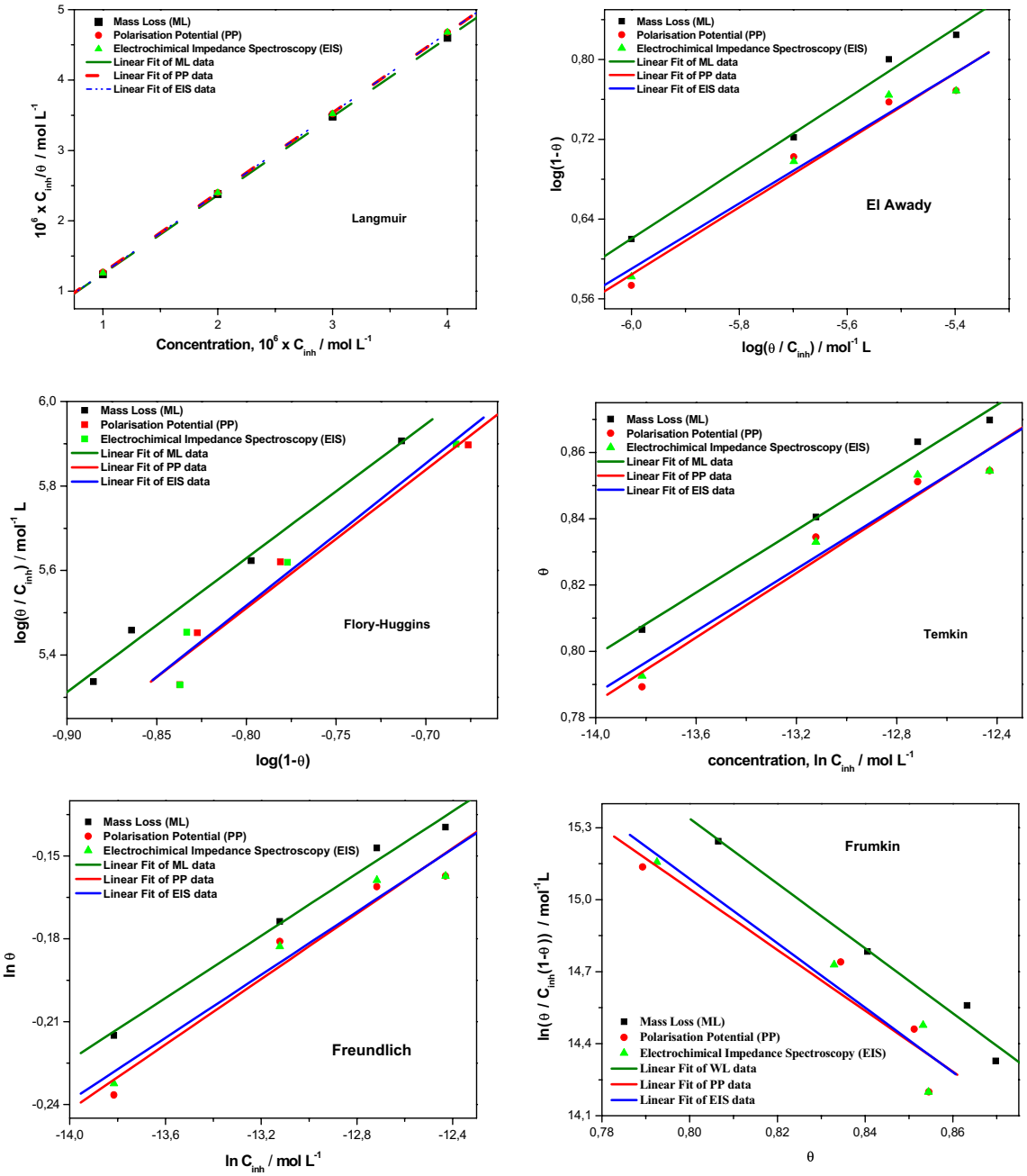

Fig. 2 Different adsorption isotherms tested for C-steel corrosion in 1.0 M HCl containing PA at 298 K

Table 3 Adsorption parameters deducted from linearizing various adsorption isotherms for C-steel corrosion in 1.0 M HCl in the presence of PA at 298 K

Isotherm	Method	R^2	K_{ads} (L mol^{-1})	$\Delta_r G_{ads}^{\circ}$ (kJ mol^{-1})	Isotherm property	
Langmuir	ML	0.9999	7.69 10^6	− 49.20	Slope	1.12
	PP	0.9999	7.69 10^6	− 49.20		1.14
	EIS	0.9999	8.33 10^6	− 49.40		1.14
El-Awady	ML	0.9914	5.81 10^7	− 54.20	1/*y*	2.84
	PP	0.9634	5.46 10^7	− 54.10		2.97
	EIS	0.9641	6.37 10^7	− 54.50		3.06
Flory–Huggins	ML	0.9904	4.59 10^7	− 53.70	*x*	3.17
	PP	0.9606	4.10 10^7	− 53.40		3.27
	EIS	0.9607	4.79 10^7	− 53.80		3.36
Temkin	ML	0.9893	2.65 10^{13}	− 86.50	*a*	− 10.60
	PP	0.9523	1.18 10^{13}	− 84.50		− 10.30
	EIS	0.9573	2.25 10^{13}	− 86.10		− 10.06
Frumkin	ML	0.9774	2.27 10^{11}	− 74.70	*a*	− 6.76
	PP	0.9021	0.87 10^{11}	− 72.40		− 6.34
	EIS	0.9122	1.65 10^{11}	− 74.00		− 6.71
Freundlich	ML	0.9844	1.7600	− 11.40	*n*	0.056
	PP	0.9492	1.8000	− 11.40		0.059
	EIS	0.9552	1.7500	− 11.30		0.057

adsorption process. Thus, El-Awady, Flory–Huggins, Temkin, Frumkin as well as Freundlich isotherms were undertaken. In the first stage, the values of the determination coefficient were very close to unity, what encouraged us to deepen more the investigation.

Indeed, the reciprocal of '*y*' obtained from El-Awady isotherm is circa 3; approximately equal to the value of size parameter '*x*' deduced from Flory–Huggins isotherm implying that three water molecules have been replaced by one PA molecule in the course of the inhibition process. Accordingly, the adsorbed species are attached to more than one active site on the metal surface in perfect disagreement with Langmuir hypothesis which stipulates that the metal surface contains a fixed number of adsorption sites and each one holds only one adsorbate inhibitor molecule. This result suggests that certain functional groups of the polymer are adsorbed on the C-steel surface while other parts of PA remain free in solution; i.e., only a certain number of segments of the long polymer chain are directly in contact with the metal surface while the other parts form lops and/or tails are in the solution. So, it can be concluded that the PA inhibitor, is probably, vertically adsorbed on the C-steel surface while the occurrence of flat adsorption by the studied compound PA may be completely ruled out. Similar results were reported by Noor [27] when studying the effect of some quaternary N-heterocyclic compounds on the corrosion of C-steel in phosphoric acid solutions.

On the other hand, the fact that the PA adsorption process also follows the Temkin and Frumkin isotherms constitutes an indication of the existence of molecular interaction in the adsorbed layer, that non-totally ideal as suggested by Langmuir isotherm. It is further confirmed by the negative sign of the intermolecular interaction parameter in the adsorption layer '*a*' of Temkin isotherm and the negative sign of the interaction parameter between molecules adsorbed on the metal surface '*a*' of Frumkin isotherm, indicating highly repulsive lateral interactions in the adsorbed layer.

From Table 3, it is clear that the value of K_{ads} obtained from different isotherms is large, except for the Freundlich isotherm model, indicating strong adsorption of PA inhibitor onto the metal surface. The values of K_{ads} and therefore of $\Delta_r G_{ads}^{\circ}$ obtained through Freundlich adsorption isotherm are, however, very low questioning the applicability of this isotherm to the system. Indeed, the '*n*' value of the Freundlich isotherm is far from the typical value of 0.6 [28], meaning that the studied adsorption process cannot be reasonably modeled by the Freundlich isotherm, despite the seemly good R^2 values obtained from the corresponding plots.

In addition, from the obtained results, the standard free-energy of adsorption has higher absolute values of $\Delta_r G_{ads}^{\circ}$ which demonstrate that the PA adsorption onto the C-steel surface is highly favored in acidic medium. $\Delta_r G_{ads}^{\circ}$ values around 40.0 kJ mol^{-1} or higher are associated with charge sharing or charge transfer from the inhibitor molecules to the metal and indicate that chemisorption is involving in the mechanism operating in the system. Furthermore, owing to the acidity of the medium, the protonation cannot be neglected and can occur, according to Fig. 3, by the reaction of the amino group with HCl. PA molecules (form II) may

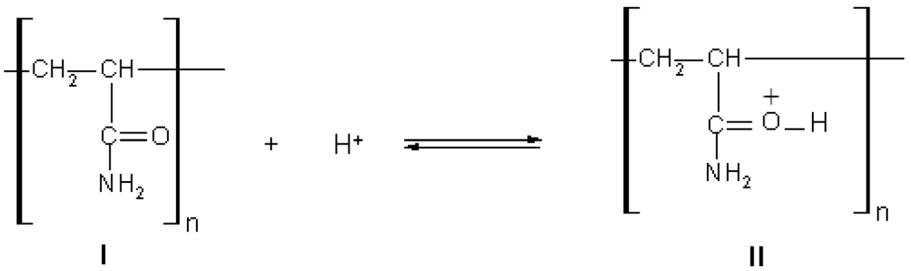

I II

Fig. 3 Protonation reaction of polyacrylamide (PA) molecules

also adsorb through electrostatic interactions between the positively charged nitrogen atoms and the negatively charged metal surface. Such protonated species are often adsorbed at cathodic sites on the metal surface and hence retard the hydrogen evolution reaction. It is noteworthy that chloride ions present in the test solution have the tendency to be specifically adsorbed on metal surface, where they facilitate adsorption of protonated inhibitor species by forming intermediate bridges between the metal surface and the inhibitor. Being specifically adsorbed, they create an excess negative charge towards the solution and favor more adsorption of the cations [29]. PA molecules may also adsorb on anodic sites through the nitrogen atoms, which are electron-donating groups, and decrease anodic dissolution of C-steel.

It may be assumed, owing to the adsorbed water molecules on the surface of C-steel that the adsorption occurs first via the electrostatic interaction, and then the removal of water molecules from the surface is accompanied by chemical interaction between the metal surface and the adsorbate as reported in reference [30]. The increase in inhibition efficiency observed with concentration of PA is because of the availability of larger number of PA molecules in both forms for adsorption, neutral and protonated, at higher concentrations up to 4×10^{-6} mol L^{-1}. The inhibiting molecules already adsorbed on the surface, start thus to desorb with increasing of PA concentration beyond 4×10^{-6} mol L^{-1}, probably because of their mutual repulsion as well as their eventual repulsion with inhibitor molecules present in solution. With increasing concentration of the PA inhibitor, these interactions become stronger, leading to the desorption which becomes more pronounced than the adsorption, that explains the observed decrease in inhibition efficiency with increase in PA inhibitor concentration above 4×10^{-6} mol L^{-1}.

Further deductions of the mechanism of inhibitor adsorption require a study of the dependence of inhibition efficiency on immersion time and temperature.

3.2 Effect of Immersion Time

The effect of immersion time constitutes an important factor in assessing the stability of inhibitive behavior of PA inhibitor. In the present study, the effect of immersion time from 0.5 to 12 h is studied at the optimum concentration of 3×10^{-6} mol L^{-1} by EIS, since this technique is not destructive and does not significantly disturb the double layer at the metal/solution interface, and therefore the results are more reliable. The Nyquist and Bode diagrams versus immersion time in uninhibited and inhibited PA inhibitor at 298 K are given in Fig. 4.

It is noted that the Nyquist diagrams exhibit one capacitive loop very similar to that obtained when varying the inhibitor concentration, attesting that there is only one-time constant whatever the immersion period. This indicates that the corrosion reaction is controlled by a charge transfer process. All the Nyquist diagrams were analyzed in terms of the same equivalent circuit, used previously, represented in Fig. 5.

The evolution of the characteristic parameters associated with this capacitive loop against time period is summarized in Table 4.

It is clearly seen from Table 4 that the increase of immersion time leads to maintenance of the inhibitory efficacy of the C-steel, at about 95.7%, even after 6 h of exposure to the aggressive solution. These results justify that the inhibitive film formed on the metal surface is very stable at higher immersion time and provides remarkable prevention against corrosion. Accordingly, the chemisorption mechanism remains the most probable process that can occur when PA inhibitor is added to the aggressive medium. Figure 6 illustrates the variation of the charge transfer resistance and double layer capacitance at different immersion time periods.

Figure 6 confirms that after 6 h of immersion, the values of R_{ct} decrease while the values of C_{dl} increase with immersion time. This supports the idea that the corrosion of C-steel is controlled by a charge transfer process [31] whose rate increases with time increase. The charge transfer resistance at 3×10^{-6} mol L^{-1} of PA changes from 257.9 Ω cm^2 after 0.5 h to 394.9 Ω cm^2 after 6 h immersion. It means that the medium corrosiveness is lowered by 1.5 times when compared to the first stage. At the same time, the capacitance values decreased from 50.74 to 21.12 μF cm^{-2}; i.e., 2.3 times more than the shortest immersion period. This evolution of R_{ct} and C_{dl} is probably due to the displacement of water molecules by the Cl^- ions of the acid and the adsorption of organic molecules onto

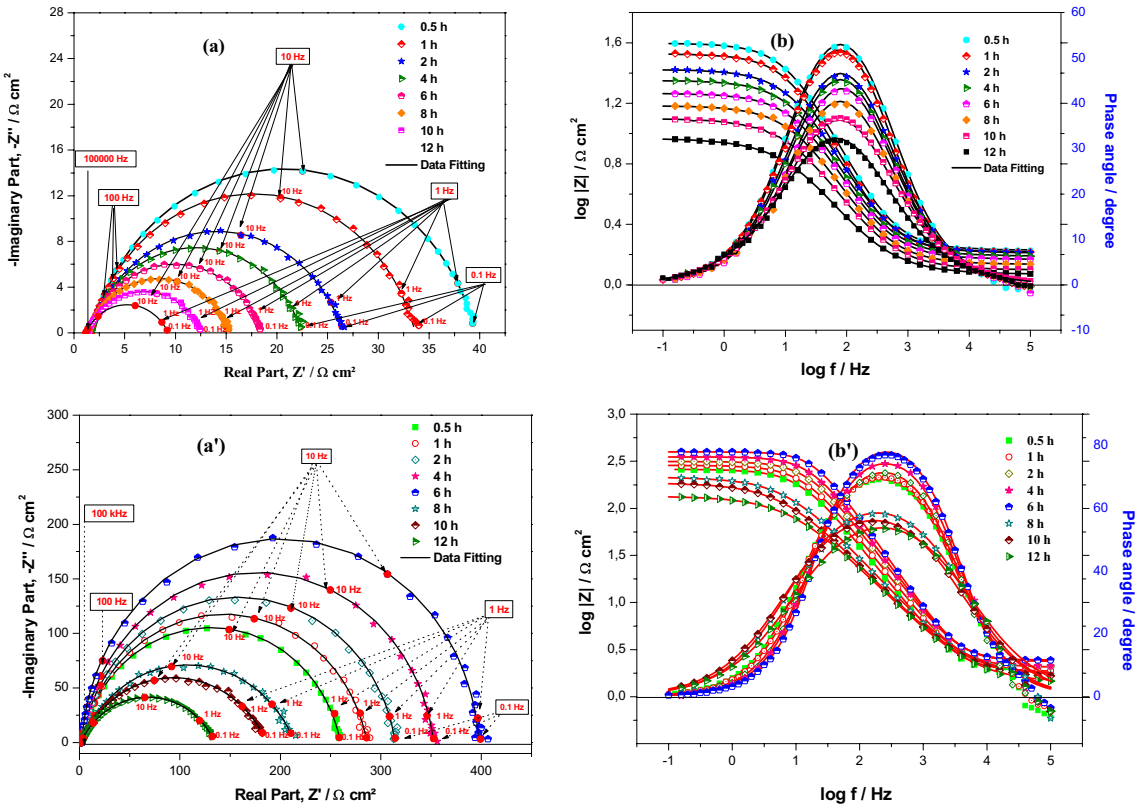

Fig. 4 Nyquist (**a, a′**) and Bode (**b, b′**) diagrams for C-steel in 1 M HCl solution at different immersion times in the absence (**a, b**) and presence (**a′**, **b′**) of PA at 3×10^{-6} mol L^{-1} and 298 K

Fig. 5 Equivalent circuit model used to fit the EIS experiment data for C-steel in 1.0 M HCl

the metal surface, decreasing the rate of metal dissolution reaction and reduction of protons H^+. These results indicate that the inhibitive action of PA may be related to its adsorption and thus formation of a barrier film on the C-steel surface.

3.3 Effect of Temperature

The temperature is an important kinetic factor that impacts the inhibition efficiency and can modify the adsorption of inhibitor on the electrode surface. In order to study the effect of this parameter on the corrosion inhibition characteristics, the experiments are conducted by both PP and EIS methods in the range of temperature from 298 to 328 K at an interval of 10 K.

3.3.1 EIS Results

The Nyquist and Bode diagrams of C-steel are obtained in 1.0 M HCl solution without and with PA at 3×10^{-6} mol L^{-1} at different temperatures and shown in Fig. 7. First, the Nyquist diagrams exhibit one capacitive loop whatever the temperature, indicating that the corrosion reaction is controlled by a charge transfer process. Electrochemical impedance parameters extracted from these diagrams, analyzed in terms of the same equivalent circuit represented in Fig. 5, are given in Table 5.

From the results given in Table 5, it can be seen that the increase of temperature reduces the values of R_{ct} and enhances those of C_{dl} or Q values both in uninhibited and inhibited solutions. However, it is to be noted that this evolution is much marked in the absence of PA inhibitor.

Table 4 Impedance data for C-steel/1.0 M HCl in the absence and presence of 3×10^{-6} mol L^{-1} of PA at 298 K and at different immersion periods

Inhibitor	Time (h)	R_s (Ω cm^2)	R_{ct} (Ω cm^2)	C_{dl} (μF cm^{-2})	Q (s^n Ω^{-1} cm^{-2})	n	η_{EIS} (%)
Blank	0.5	1.676	37.86	364.1	763	0.8273	–
	1	1.658	32	402.4	860	0.8255	–
	2	1.626	24.9	470.8	1200	0.7892	–
	4	1.551	20.95	522.8	1360	0.7887	–
	6	1.474	16.98	563.1	1530	0.7846	–
	8	1.368	13.96	708.7	2130	0.7614	–
	10	1.259	11.31	901.2	3190	0.7243	–
	12	1.176	8.115	1292	5150	0.6966	–
PA	0.5	1.857	257.9	50.74	88	0.8730	85.3
	1	2.060	284.1	41.97	71.2	0.8807	88.7
	2	2.105	311.9	32.43	51.2	0.9007	92
	4	2.129	349.9	26.79	37.7	0.9266	94
	6	2.452	394.9	21.12	25	0.9649	95.7
	8	1.733	212.3	98.49	257	0.752	93.4
	10	1.613	183.3	129.6	349	0.7354	93.8
	12	1.421	133.5	132.5	428	0.7094	93.9

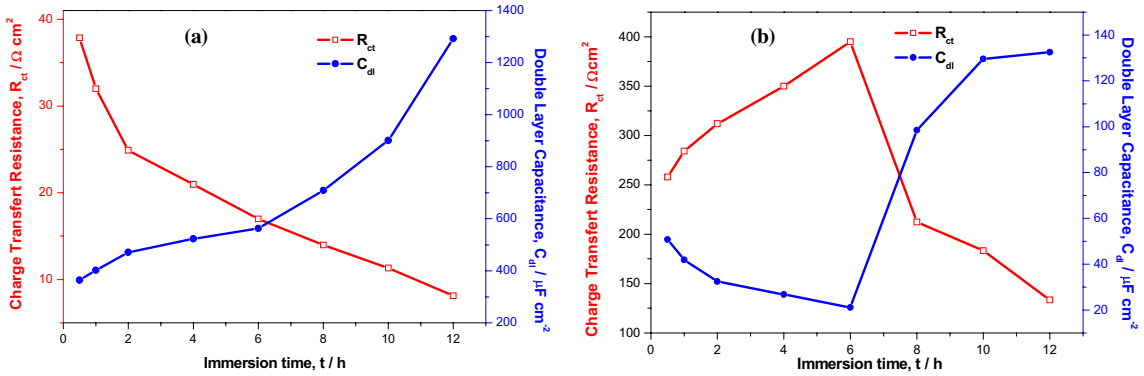

Fig. 6 Variation of charge transfer resistance R_{ct} and double layer capacitance C_{dl} versus immersion time at 298 K in the absence (**a**) and in the presence (**b**) of 3×10^{-6} mol L^{-1} of PA

These results confirm that PA acts as an efficient inhibitor for C-steel in 1.0 M HCl in the range of the studied temperature.

It is also observed from Table 5 that the inhibition efficiency is improved significantly from 308 to 318 K. It can be suggested that PA inhibitor molecules block the surface of C-steel via adsorption mechanism. The observed improvement in inhibition efficiency with rise of temperature can be attributed to a change in the nature of adsorption, wherein the inhibitor molecules is physically adsorbed at lower temperature whilst protonated inhibitor species, chemisorption is favored at higher temperature. In our case, the fact that the inhibition efficiency remains constant if not ameliorate when temperature increases beyond 318 K suggests that the inhibitor film becomes more compact and protective.

3.3.2 Potentiodynamic Polarization Results

The influence of temperature on the inhibition efficiency of PA is also studied by potentiodynamic polarization. The steady-state curves obtained for C-steel in 1.0 M HCl without and with 3×10^{-6} mol L^{-1} of PA inhibitor in the temperature range 298–328 K are shown in Fig. 8. Electrochemical parameters extracted from these curves are given in Table 6.

As can be seen from Table 6, it is apparent that the increase of current density is much pronounced with the rise of temperature in the uninhibited solutions than in the inhibited solution. The observed increase in the inhibition efficiency of PA from 303 to 318 K suggests again that the molecules may be chemically adsorbed on the metal surface. However, the slight decrease in inhibition efficiency observed is an indication that protonated PA

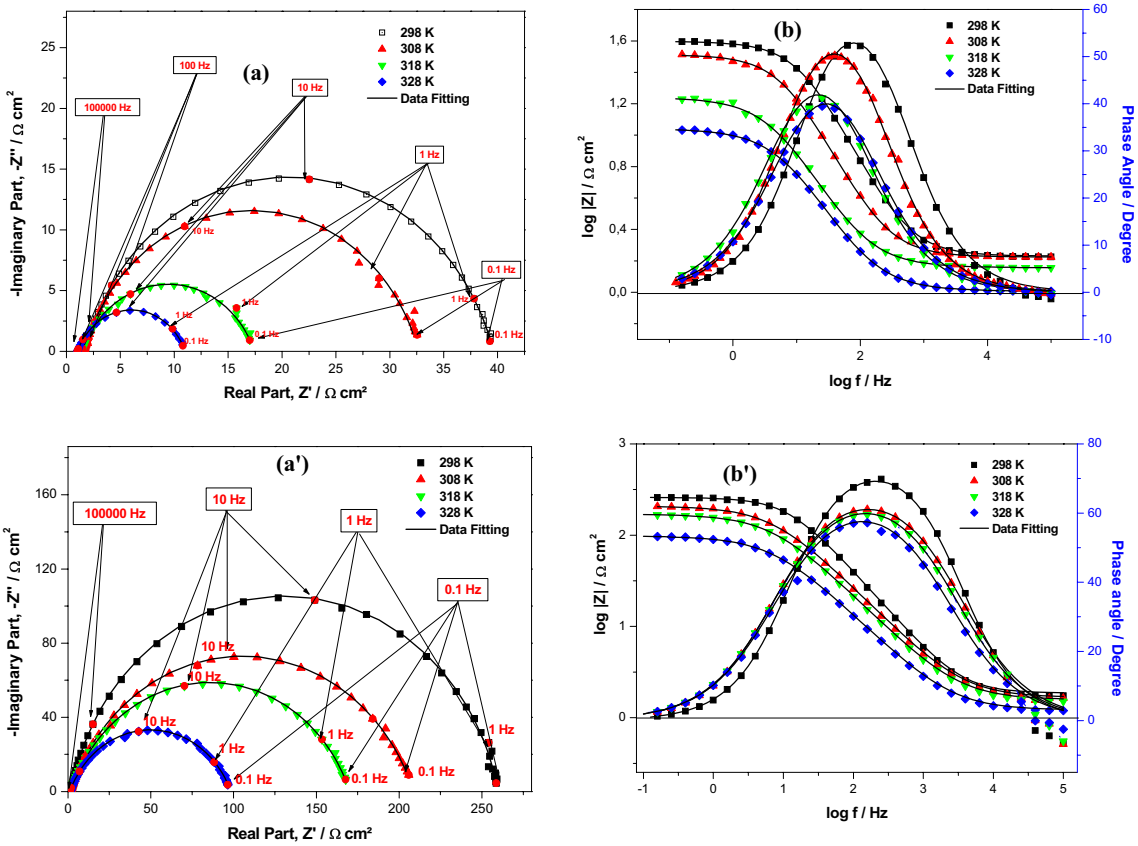

Fig. 7 Nyquist (**a, a′**) and Bode (**b, b′**) diagrams for C-steel in 1 M HCl solution at different temperatures in the absence (**a, b**) and presence of PA at 3×10^{-6} mol L^{-1} (**a′**, **b′**) and at 298 K

Table 5 Electrochemical impedance parameters for C-steel in 1.0 M HCl in the absence and presence of 3×10^{-6} mol L^{-1} PA at different temperatures

Inhibitor	T (K)	R_s (Ω cm^2)	R_{ct} (Ω cm^2)	C_{dl} (μF cm^{-2})	Q (s^n Ω^{-1} cm^{-2})	n	η_{EIS} (%)
Blank	298	1.676	37.86	364.1	763	0.8273	–
	308	1.673	30.99	804.4	1570	0.8185	–
	318	1.432	16.01	2304	4920	0.7699	–
	328	1.016	10.00	2636	6280	0.7613	–
PA	298	1.857	257.9	50.74	88	0.8730	85.3
	308	1.664	207.1	104.1	240	0.7824	85.0
	318	1.570	168.6	130.2	306	0.7761	90.5
	328	1.207	97.06	216.5	536	0.7650	89.7

species can also be absorbed by electrostatic interaction with chloride ion already adsorbed on the iron surface. This is further confirmed from the enhancing values obtained of inhibition efficiency. Therefore, it is concluded that the adsorption of PA molecules is a mixed type of chemical and physical adsorptions, and that the chemical interactions should be dominant for the adsorption of PA molecules on the C-steel surface.

3.3.3 Activation Parameters of C-Steel Dissolution

The activation energy for C-steel dissolution in the absence and the presence of PA is calculated from both corrosion current density (E_a) and charge transfer resistance (E_a') using the Arrhenius expression, in logarithmic form, Eqs. (7) and (8):

$$\ln\left(i_{corr}\right) = \ln A - (E_a/RT) \tag{7}$$

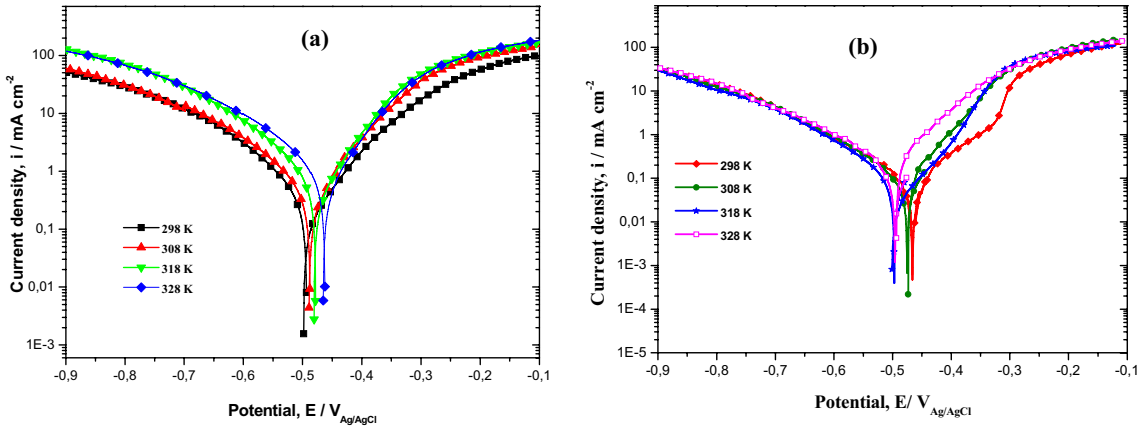

Fig. 8 Polarization curves at different temperatures for C-steel **a** in the absence of PA and **b** in the presence of PA at 3×10^{-6} mol L^{-1}

Table 6 Polarization parameters for C-steel corrosion in 1.0 M HCl in the absence and presence of PA at 3×10^{-6} mol L^{-1} at different temperatures

Inhibitor	T (K)	$^{-}E_{corr}$ ($mV_{Ag/AgCl}$)	$^{-}\beta_c$ (mV dec^{-1})	i_{corr} (μA cm^{-2})	η_{PP} (%)
Blank	298	495	168	598	–
	308	487	173	731	–
	318	477	164	1421	–
	328	462	193	2298	–
PA	298	465.5	136	89	85.1
	308	476.5	138.8	110	84.9
	318	498.1	172.7	133	90.6
	328	497.5	159.5	232	89.9

$$\ln\ (1/R_{ct}) = \ln A' - (E_a'/RT) \tag{8}$$

where A, A' are the Arrhenius pre-exponential factors.

Plots of the natural logarithm of corrosion current density i_{corr} and of $1/R_{ct}$ versus $1/T$ are given in Fig. 9. The E_a and values obtained from the slope and the intercept, respectively, of the Arrhenius plots are given in Table 7.

The enthalpy and entropy of C-steel dissolution process may also be evaluated from the temperature effect from the alternatives formulations of Arrhenius equations, taken in logarithmic form (9) and (10).

$$\ln\ \left(i_{corr}/T\right) = (\Delta S*/R) + \ln\ (R/N\,h) + (-\Delta H*/RT) \tag{9}$$

$$\ln\ (1/R_{ct}T) = (\Delta S*/R) + \ln\ (R/N\,h) + (-\Delta H*/RT) \tag{10}$$

where h is Planck's constant ($h = 6.6252\ 10^{-34}$ J s); N is Avogadro's number ($N = 6.023\ 10^{23}$ mol^{-1}); $\Delta S*$ is the entropy of activation and $\Delta H*$ is the enthalpy of activation.

Straight lines are obtained from Fig. 9 with a slope of $(-\Delta H*/R)$ and an intercept of $(\Delta S*/R) + ln\ (R/N\,h)$ from which the values of $\Delta H*$ and $\Delta S*$ are calculated and also listed in Table 7.

It should first be noted, as shown in Table 7, that the results obtained from potentiodynamic polarization data are in good agreement with those obtained from EIS measurements. The activation energy value in the presence of PA is lower than the one in uninhibited solution. In the same way, the pre-exponential factor A decreases dramatically in the presence of PA. The decrease of E_a as well as A in the presence of PA indicates the easier adsorption of PA on C-steel surface. This observation further supports the proposed chemisorption mechanism. Indeed, unchanged or lowered E_a in inhibited systems when compared to the blank has been reported to be indicative of chemical adsorption mechanism, while increased E_a suggests a physical adsorption mechanism. On the other hand, the decrease of activation energy accompanying the increase the inhibition efficiency of PA, previously observed (Table 5), at higher temperatures is due to the changing nature of the adsorption. These results provide evidence that the adsorption of PA onto the surface of C-steel is of mixed interactions: predominant chemisorption and weak physisorption.

It is shown in Table 7 that the values of E_a and $\Delta H*$ are close to each other as expected from the concept transition

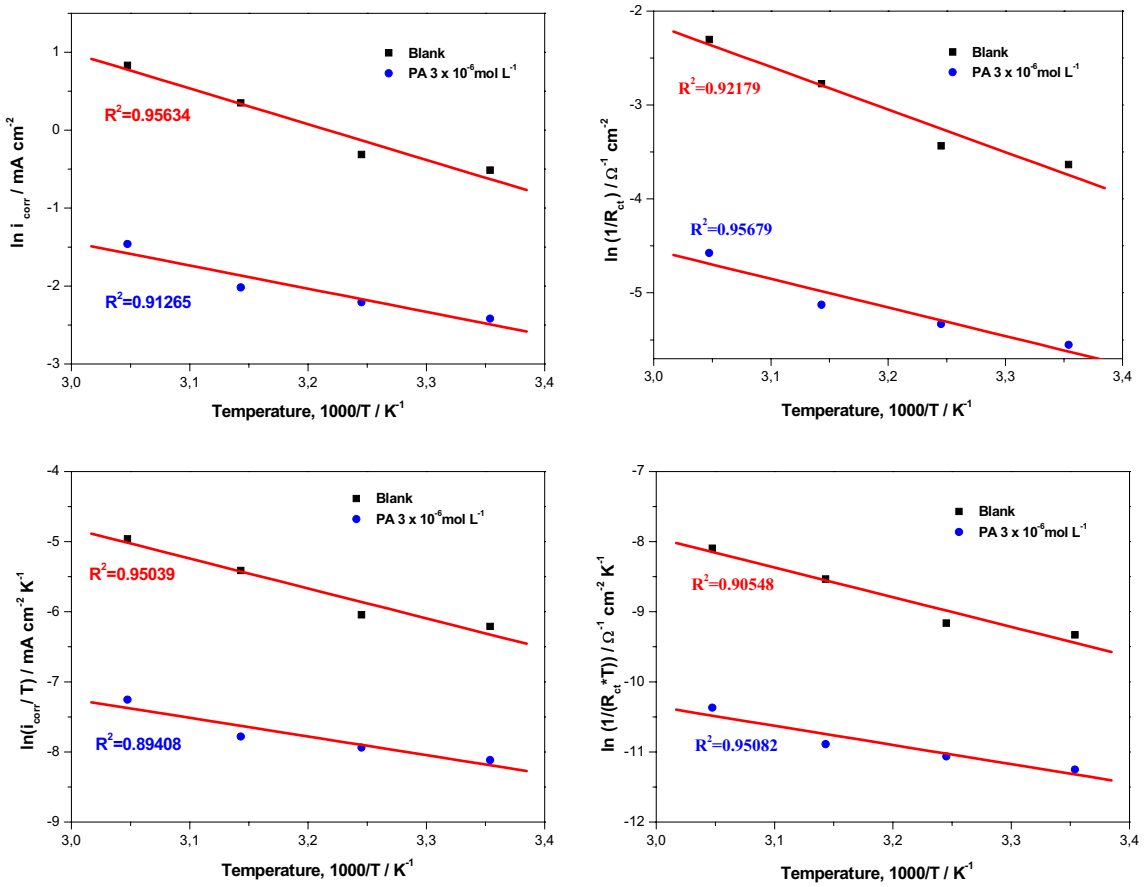

Fig. 9 Arrhenius plots of C-steel obtained in 1.0 M HCl in the absence (filled square) and presence (filled circle) of 3×10^{-6} mol L^{-1} of PA obtained from EIS and PP measurements

Table 7 Activation parameters for C-steel in 1.0 M HCl in the presence and the absence of 3×10^{-6} mol L^{-1} of PA obtained from electrochemical and potentiodynamic polarization measurements

Kinetic parameter	Method	A	E_a (kJ mol^{-1})	ΔH^* (kJ mol^{-1})	ΔS^*(J K^{-1} mol^{-1})	$E_a - \Delta H^*$ (kJ mol^{-1})
Blank	EIS	9.4×10^4	37.70	35.10	−46.24	2.60
	PP	2.5×10^6	38.10	35.50	−73.74	2.60
PA	EIS	1.1×10^2	25.33	22.75	−102.64	2.58
	PP	1.7×10^3	24.69	22.11	−133.23	2.58

state theory and vary in the same manner on the addition of inhibitor. This result permits to verify the well-known thermodynamic relation between E_a and ΔH^* as shown in Eq. (11):

$$E_a - H^* = R\,T \tag{11}$$

The calculated value of the difference (Table 7) is close to the experimental value of RT, i.e., 2.56 kJ mol^{-1} at 308 K. On the other hand, the positive sign of the enthalpy ΔH^* in the absence and presence of inhibitor reflects the endothermic nature of the metal dissolution process, which suggests the slow dissolution of C-steel. The entropy of activation ΔS^* in the absence and presence of the inhibitor are larges negative. This indicates that the activated complex in the rate determining step which represents an association rather than a dissociation step, meaning that, a decrease in disordering is taking place on going from reactants to the activated complex.

4 Conclusion

From the above analyses and discussion of the kinetic–thermodynamic parameters, the following main conclusions can be drawn:

1. The overall data suggest that the corrosion inhibition takes place by adsorption of the PA molecules on the C-steel surface through both chemical and physical interactions and this adsorption is a spontaneous and endothermic process accompanied by a decrease in entropy.
2. The adsorption of PA on C-steel surface is characterized by negative interaction coefficients of Frumkin and Temkin isotherms, indicating repulsive lateral interactions in the adsorbed inhibitor layer.
3. According to Flory–Huggins isotherm and the kinetic–thermodynamic model of El-Awady, three water molecules are displaced and replaced by one PA molecule.
4. The inhibition efficiency remains stable around 90% despite the increase of temperature till 328 K.
5. The corrosion rate of C-steel in 1.0 M HCl solution without and with PA depends on immersion time from 0.5 to 12 h, with an optimum result registered at the 6th hour of exposure.

Funding This study was supported by BENIKEN.

References

1. Rajendran S, Sridevi SP, Anthony N, John Amalraji A, Sundaravadivedi M (2005) Corrosion behavior of carbon steel in polyvinyl alcohol. Anti-Corros Methods Mater 52:102–107. https://doi.org/10.1108/00035590510584816
2. Umoren SA, Lia Y, Wang FH (2010) Electrochemical study of corrosion inhibition and adsorption behaviour for pure iron by polyacrylamide in H_2SO_4: synergistic effect of iodide ions. Corros Sci 52:1777–1786. https://doi.org/10.1016/j.corsci.2010.01.026
3. Umoren SA, Obot IB (2008) Polyvinylpyrollidone and polyacrylamide as corrosion inhibitors for mild steel in acidic medium. Surf Rev Lett 15:277–286. https://doi.org/10.1142/S0218625X08011366
4. Amin MA, EI-Rehim SS, El-Sherbini EE, Hazzazi OA, Abbas MN (2009) Polyacrylic acid as a corrosion inhibitor for aluminium in weakly alkaline solutions. Part I: weight loss, polarization, impedance EFM and EDX studies. Corros Sci 51:658–667. https://doi.org/10.1016/j.corsci.2008.12.008
5. Finšgar M, Fassbender S, Nicolini F, Milošev I (2009) Polyethyleneimine as a corrosion inhibitor for ASTM 420 stainless steel in near-neutral saline media. Corros Sci 51:525–533. https://doi.org/10.1016/j.corsci.2008.12.006
6. Gupta G, Birbilis N, Khanna (2013) Polyaniline–lignosulfonate/epoxy coating for corrosion protection of AA2024-T3. Corros Sci 67:256–267. https://doi.org/10.1016/j.corsci.2012.10.022
7. Chetouani A, Medjahed K, Al-Deya SS, Hammouti B, Warad I, Mansri A, Aouniti A (2012) Inhibition of corrosion of pure iron by quaternized poly(4-vinylpyridine)-graft-bromodecane in sulphuric Acid. Int J Electrochem Sci 7:6025–6043
8. Arthur DE, Jonathan A, Ameh PO, Anya C (2013) A review on the assessment of polymeric materials used as corrosion inhibitor of metals and alloys. Int J Ind Chem 4:2–9. https://doi.org/10.1186/2228-5547-4-2
9. Saliyan VR, Adhikari AV (2008) Inhibition of corrosion of mild steel in acid media by N′-benzylidene-3-(quinolin-4-ylthio) propanohydrazide. Bull Mater Sci 31:699–711. https://doi.org/10.1007/s12034-008-0111-4
10. Benabdellah M, Ousslim A, Hammouti B, Elidrissi A, Aouniti A, Dafali A, Bekkouch K, Benkaddour M (2007) The effect of poly(vinyl caprolactone-co-vinyl pyridine) and poly(vinyl imidazol-co-vinyl pyridine) on the corrosion of steel in H_3PO_4 media. J Appl Electrochem 37:819–826. https://doi.org/10.1007/s10800-007-9317-1
11. Müller LB, Schmelich T (1995) High-molecular weight styrene maleic acid copolymers as corrosion inhibitors for aluminium pigments. Corros Sci 37:877–883. https://doi.org/10.1016/0010-938X(94)00171-2
12. Bereket G, Yurt A, Turk H (2003) Inhibition of corrosion of low carbon steel in acidic solution by selected polyelectrolytes and polymers. Anti-Corros Methods Mater 50:422–435. https://doi.org/10.1108/00035590310501585
13. Umoren SA, Ogbobe O, Okafor PC, Ebenso EE (2007) Polyethylene glycol and polyvinyl alcohol as corrosion inhibitors for aluminium in acidic medium. J Appl Polym Sci 105:3363–3370. https://doi.org/10.1002/app.26530
14. Shukla SK, Quraishi MA, Prakash R (2008) A self-doped conducting polymer polyanthranilic acid an efficient corrosion inhibitor for mild steel in acidic solution. Corros Sci 50:2867–2872 https://doi.org/10.1016/j.corsci.2008.07.025
15. Ren Y, Luo Y, Zhang K, Zhu G, Tan X (2008) Lignin terpolymer for corrosion inhibition of mild steel in 10% hydrochloric acid medium. Corros Sci 50:3147–3153. https://doi.org/10.1016/j.corsci.2008.08.019
16. Solomon MM, Umoren SA, Udosoro II, Udoh AP (2010) Inhibitive and adsorption behaviour of carboxymethyl cellulose on mild steel corrosion in sulphuric acid solution. Corros Sci 52:1317–1325. https://doi.org/10.1016/j.corsci.2009.11.041
17. Umoren SA, Li Y, Wang FH (2011) Influence of iron microstructure on the performance of polyacrylic acid as corrosion inhibitor in sulfuric acid solution. Corros Sci 53:1778–1785. https://doi.org/10.1016/j.corsci.2011.01.052
18. Bhandari H, Srivastav R, Choudhary V, Dhawan SK (2010) Enhancement of corrosion protection efficiency of iron by poly(aniline-co-amino-naphthol-sulphonic acid) nanowires coating in highly acidic medium. Thin Solid Films 519:1031–1039. https://doi.org/10.1016/j.tsf.2010.08.038
19. Yurt A, Buetuen V, Duran B (2007) Effect of the molecular weight and structure of some novel water-soluble triblock copolymers on the electrochemical behaviour of mild steel. Mater Chem Phys 105:114–121. https://doi.org/10.1016/j.matchemphys.2007.04.009
20. Abd El-Maksoud SA, Fouda AS (2005) Some pyridine derivatives as corrosion inhibitors for carbon steel in acidic medium. Mater Chem Phys 93:84–90. https://doi.org/10.1016/j.matchemphys.2005.02.020
21. Zerga B, Hammouti B, Ebn Touhami B, Touir R, Taleb M, Sfaira M, Bennajeh M, Forssal I (2012) Comparative inhibition study of new synthesized pyridazine derivatives towards mild steel corrosion in hydrochloric acid. Part-II: thermodynamic proprieties. Int J Electrochem Sci 7:471–483
22. Singh AK, Quraish MA (2011) Investigation of the effect of disulfiram on corrosion of mild steel in hydrochloric acid solution. Corros Sci 53:1288–1297. https://doi.org/10.1016/j.corsci.2011.01.002
23. Migahed MA, Farag AA, Elsaed SM, Kamal R, Mostfa M, Abd El-Bary H (2011) Synthesis of a new family of Schiff base nonionic surfactants and evaluation of their corrosion inhibition effect on X-65 type tubing steel in deep oil wells formation water. Mater Chem Phys 125:125–135. https://doi.org/10.1016/j.matchemphys.2010.08.082

24. Bockris JOM, Khan SUM (1970) Surface electrochemistry: a molecular level approach. Plenum, New York. ISBN 978-1-4615-3040-4
25. Fu J, Pan J, Liu Z, Li S, Wang Y (2011) Corrosion inhibition of mild steel by benzopyranone derivative in 1.0 M HCl solutions. Int J Electrochem Sci 6:2072–2089
26. Andreani S, Znini M, Paolini J, Majidi L, Hammouti B, Costa J, Muselli A (2016) Study of corrosion inhibition for mild steel in hydrochloric acid solution by *Limbarda crithmoides* essential oil of Corsica. J Mater Environ Sci 7(1):187–195
27. Noor EA (2005) The inhibition of mild steel corrosion in phosphoric acid solutions by some N-heterocyclic compounds in the salt form. Corros Sci 47:33–55. https://doi.org/10.1016/j.corsci.2004.05.026
28. Khadom AA. Yaro AS, Kadhum AAH (2010) Adsorption mechanism of benzotriazole for corrosion inhibition of copper–nickel alloy in hydrochloric acid. J Chil Chem Soc 55:150–152 dx. https://doi.org/10.4067/S0717-97072010000100035
29. Iofa ZA, Tomashov GN (1963) Joint action of hydrogen sulfide and organic compounds on corrosion and embrittlement of iron in sulfuric acid. Corrosion 19(1):12t–16t. https://doi.org/10.5006/0010-9312-19.1.12
30. Shaw DJ (2013) Introduction to colloid and surface chemistry, 4th edn. Butterworth-Heinemann, Oxford. ISBN 978-0-08-050910-5
31. Bentiss F, Traisne M, Gengembre L, Lagrenée M (1999) A new triazole derivative as inhibitor of the acid corrosion of mild steel: electrochemical studies, weight loss determination, SEM and XPS. Appl Surf Sci 152:237–249. https://doi.org/10.1016/S0169-4332(99)00322-0